Microbial Cell Factories

RESEARCH Open Access

Enhanced Natamycin production in *Streptomyces gilvosporeus* through phosphate tolerance screening and transcriptome-based analysis of high-yielding mechanisms

Liang Wang[1], Wen Xiao[1], Ting Qiu[1], Hongjian Zhang[1], Jianhua Zhang[1] and Xusheng Chen[1*]

Abstract

Background Natamycin is a natural antibiotic with broad-spectrum antifungal activity, widely used in food preservation, medicine, and biological control. However, the relatively low biosynthetic capacity of producing strains limits further industrialization and broader applications of natamycin. Due to the complexity of cellular metabolism, evolutionary engineering is required for developing strains with enhanced natamycin biosynthetic capacity.

Results Here, protoplast fusion combined with phosphate tolerance screening was employed for the first time to enhance natamycin production of *Streptomyces gilvosporeus*. A high-yielding strain, GR-2, was obtained, with natamycin production twice that of the original strain. Transcriptomic analysis revealed that the natamycin biosynthetic gene cluster and several primary metabolic pathways were significantly upregulated in GR-2, likely contributing to its high production performance. Further experiments, including amino acid addition and reverse engineering, confirmed that branched-chain amino acid, nitrogen, and phosphate metabolism play crucial roles in promoting natamycin production. Silencing of the phosphate metabolism transcriptional regulators PhoP and PhoR led to a decreased expression of natamycin biosynthetic genes and significantly reduced natamycin production, highlighting the key role of these regulators in *S. gilvosporeus*. Based on omics data, co-expression of *phoP* and *phoR* in GR-2 resulted in the engineered strain GR2-P3, which exhibited a 25% increase in natamycin production in shake flasks. In a 5 L fermenter, GR2-P3 achieved a natamycin production of 12.2 ± 0.6 g·L^{-1}, the highest yield reported for *S. gilvosporeus* to date.

Conclusions Our findings suggest that the high production performance of GR-2 is primarily due to the upregulation of the natamycin biosynthetic gene cluster and genes related to precursor supply. Increasing the intracellular supply of valine and glutamate significantly enhanced natamycin production. Additionally, the natamycin biosynthetic gene cluster is likely positively regulated by PhoP and PhoR. Our work presents a novel strategy for

*Correspondence:
Xusheng Chen
chenxs@jiangnan.edu.cn

Full list of author information is available at the end of the article

strain screening and evolution to improve natamycin production and identifies novel molecular targets for metabolic engineering.

Keywords Natamycin, *Streptomyces gilvosporeus*, Phosphate-tolerance screening, Comparative transcriptomics, Transcriptional regulation

Background

Natamycin is a natural polyene macrolide antibiotic characterized by a unique 26-membered lactone ring structure with four conjugated double bonds. This structure enables it to bind to ergosterol in fungal cell membranes at low concentrations, thereby exhibiting potent broad-spectrum antifungal activity [1]. Natamycin is poorly soluble in water but is easily soluble in organic solvents. When stored as a powder under light-protected conditions, it remains stable for extended periods without loss of activity. Due to its low toxicity in mammalian cells, natamycin has been approved as a natural food preservative in over 40 countries. Additionally, natamycin can be used in the medical field for antifungal infections and cancer treatment and in agriculture as a crop protection agent to prevent fungal contamination [2, 3]. According to statistics, the global annual production of natamycin was $61 million in 2021 and is expected to exceed $100 million by 2032 (https://www.futuremarketinsights.com, accessed 14 Jan. 2025). Despite the high marke t demand, the industrial production of natamycin still faces the challenges of high production costs and low efficiency [4].

Natamycin is primarily synthesized by aerobic submerged fermentation using several species of *Streptomyces*, including *Streptomyces gilvosporeus, Streptomyces natalensis, Streptomyces chattanoogensis*, and *Streptomyces lydicus* [5]. Given its commercial value, numerous studies have attempted to optimize the fermentation process to increase natamycin production and reduce costs. For instance, adding oil as a precursor during fermentation can increase natamycin production to 7 $g{\cdot}L^{-1}$ within 8 days, which is the highest production reported to date [6]. In addition to precursor feeding, other methods, such as adding fungal inducers [7], optimizing fermentation conditions [5, 8], controlling cell morphology [9], and employing cell immobilization [10], have been effective in improving natamycin production. However, the synthetic efficiency of natamycin-producing strains remains relatively low, limiting further increases in production through fermentation process optimization [11].

Traditional methods (such as physicochemical mutagenesis and streptomycin resistance screening) are commonly used to enhance natamycin fermentation performance [12]. For example, Sun et al. utilized ultraviolet (UV), atmospheric and room temperature plasma (ARTP), and diethyl sulfate (DES) mutagenesis to obtain a high-yielding mutant, DES-26, which produced 1.64 $g{\cdot}L^{-1}$ of natamycin, an increase of 86.36% over the original strain [13]. However, these methods usually induce mutations in only a limited number of genes, which can be restrictive and time-consuming for evolving strains toward the ideal phenotype. Genetic engineering is also an effective method for enhancing secondary metabolite biosynthesis. Research has shown that natamycin is primarily synthesized from acetyl-CoA and methylmalonyl-CoA by a multifunctional polyketide synthase system [14]. Overexpression of cholesterol oxidase using a strong promoter (P*ermE**) can increase natamycin production and biomass by 72% and 81%, respectively [15]. Heterologous expression of the transcription regulatory factor AfsRS in *S. gilvosporeus* TZ1401 enhanced natamycin production by increasing the transcription of genes within the natamycin biosynthetic gene cluster (BGC) [16]. However, due to the complexity of cellular metabolism, the regulatory mechanisms of natamycin synthesis remain unclear, limiting metabolic engineering efforts to improve the efficiency of natamycin synthesis.

Protoplast fusion is an effective tool for rapid strain improvement. The advantage of this technique lies in its ability to induce changes at multiple genomic locations simultaneously, making it a practical method for quickly integrating complex phenotypes without detailed genetic background of microorganisms [17]. This technique has been successfully applied to enhance the production efficiency of secondary metabolites in actinomycetes by increasing the yield of undecylprodigiosin in *Streptomyces* spp. ALAA-R20 and vincamine in *Streptomyces hygroscopicus* [18, 19]. In addition, phosphate is essential for microbial growth; however, natamycin biosynthesis is highly sensitive to phosphate regulation [20]. When phosphate concentrations exceed 1 mM, natamycin production declines sharply, and at 10 mM, the expression of biosynthetic genes is entirely repressed [21]. Therefore, enhancing the phosphate tolerance of natamycin-producing strains may alleviate this inhibitory effect, allowing the strain to grow and produce natamycin even under high phosphate concentrations.

The aim of this study is to enhance natamycin production in *Streptomyces gilvosporeus* by combining protoplast fusion, phosphate tolerance screening, and transcriptomic analysis, providing insights into high-yielding mechanisms and identifying novel targets for metabolic engineering. Here, protoplast fusion combined with phosphate tolerance screening was first utilized for increasing natamycin production. Subsequently,

comparative transcriptomics was used to identify the potential key metabolic pathways and genetic elements that lead to high natamycin production. These findings were validated by amino acid addition, gene overexpression, and gene silencing experiments, and natamycin production was further improved using a cooperative gene overexpression strategy. These insights not only provided an effective evolutionary engineering strategy for enhancing natamycin production, but also enhanced our understanding of the global and specific regulatory mechanisms of the natamycin biosynthetic pathway, identified potential molecular targets for metabolic engineering, and facilitated strain improvement.

Materials and methods

Media and culture conditions

S. gilvosporeus ATCC13326 was used as the original strain. Sporulation was induced by cultivating the strain on MS medium (composed of 20 g·L^{-1} mannitol, 20 g·L^{-1} soybean flour, and 20 g·L^{-1} agar, with natural pH) at 28 °C for 8–10 days. Seed medium (M3G) consisted of 5 g·L^{-1} yeast extract, 50 g·L^{-1} glucose, 10 g·L^{-1} $(NH_4)_2SO_4$, 1.36 g·L^{-1} KH_2PO_4, 0.8 g·L^{-1} K_2HPO_4, 0.5 g·L^{-1} $MgSO_4$·7 H_2O, 0.04 g·L^{-1} $ZnSO_4$·7 H_2O, and 0.03 g·L^{-1} $FeSO_4$·7 H_2O, with the pH adjusted to 7.0. Fermentation medium was composed of 20 g·L^{-1} soy peptone, 4.5 g·L^{-1} yeast extract, 2 g·L^{-1} NaCl, 1 g·L^{-1} $MgSO_4$·7 H_2O, and 60 g·L^{-1} glucose, with the pH also adjusted to 7.0.

For shake flask fermentation, 100 µL of spore suspension was inoculated into 30 mL of M3G medium in a 250 mL flask and incubated at 28 °C and 220 r·min^{-1} for 24 h. Then, 1.8 mL of the seed culture was transferred into another flask with 30 mL of M3G medium for further incubation. Finally, 1.8 mL of seed culture was transferred to 30 mL of fermentation medium and fermented at 28 °C and 220 r·min^{-1} for 4 days. If required, kanamycin, apramycin, chloramphenicol, and nalidixic acid were supplemented into the aforementioned media at final concentrations of 25, 50, 25, and 25 µg·mL^{-1}, respectively. *Escherichia coli* strain DH5α was used for plasmid isolation and cultured in Luria–Bertani medium (tryptone 10 g·L^{-1}, yeast extract 5 g·L^{-1}, NaCl 10 g·L^{-1}) at 37.0 °C and at 200 rpm.

Fed-batch fermentation was performed at 28 °C in a 5 L bioreactor (Baoxing Co., Shanghai, China) with an initial working volume of 3.5 L and 6% (v/v) inoculation. Airflow was set at 1 vvm, dissolved oxygen (DO) was maintained above 20% by adjusting the aeration and rotation speeds, and pH was kept at 6.0 using ammonia water. Glucose was supplemented when its concentration dropped below 20 g·L^{-1}.

Strains and plasmids construction

The strains, plasmids, and primers used in this study are listed in Tables S1 and S2. To construct plasmids for overexpression, the target genes (*nasA*, *nasB*, *gdhA*, *nirB*, *phoP* and *phoR*) were cloned by PCR amplification from the genome of *S. gilvosporeus* ATCC13326, and the obtained fragments were purified and ligated into the linearized vector pIB139. Subsequently, the transformed cells were introduced into *E. coli* DH5α competent cells, and the transformants were selected on amphotericin-resistant plates overnight. Plasmids were isolated and validated by colony PCR to obtain overexpression plasmids. To construct gene silencing plasmids, the P*ermE**, *hfq*, and *micC* fragments were amplified from the *E. coli* E12 genome and the terminator *to* was amplified from the pAcas9 plasmid. P*ermE**and *hfq* were ligated into the *EcoRI* linearized pIB139 vector using a one-step cloning kit, to obtain the recombinant plasmid pIB139-*hfq*. Subsequently, *micC* and *to* were ligated to the linearized pIB139-*hfq* vector and treated with *NdeI* and *EcoRV* to obtain the recombinant plasmid pIB139-*hfq-micC*. The 24 bp *anti-phoP* and *anti-phoR* fragments were ligated to *NdeI*-treated pIB139-*hfq-micC* to obtain the final recombinant plasmid.

Finally, the recombinant plasmids were transformed into *E.coli* ET12567, and transferred by conjugation to *S. gilvosporeus* ATCC13326. They were then plated on MS medium plates containing ampicillin and nalidixic acid for ex-conjugant selection. After mycelial growth, colony PCR was performed for verification. This resulted in the overexpression of *nasA*, *nasB*, *gdhA*, *nirB*, *phoP*, and *phoR*, as well as *phoP* or *phoR* antisense RNA.

ARTP, DES mutagenesis, and protoplast fusion

For ARTP mutagenesis, the spore suspension (10^8 CFU/mL) of *S. gilvosporeus* ATCC13326 was diluted 10-fold with sterile water, and 10 µL was spread evenly on a sterile mutagenic slide. Mutagenesis was performed under the following conditions: operating voltage of 100 W, irradiation distance of 2 mm, air flow rate of 10 L/min, and irradiation times of 0, 40, 60, 80, 100, and 120 s. After mutagenesis, the slide was placed in a centrifuge tube containing 1.5 mL of sterile water, and the spores were washed using a pipette. The resulting suspension was diluted 10-fold and spread on MS medium, followed by incubation at 28 °C in an inverted position. At the end of incubation, colony growth and mortality rates were recorded. For DES mutagenesis, 1 mL of the spore suspension was added to a 15 mL centrifuge tube, followed by 9 mL of PBS buffer and 0.1 mL of DES to achieve a final concentration of 1% DES solution. The reaction was terminated by adding 0.5 mL of 25% sodium thiosulfate after treatment at 28 °C for 0, 10, 20, 30, 40, and 60 min. The treated spore suspension was then diluted 100-fold,

spread onto MS medium, and incubated at 28 °C in an inverted position. Colony growth and lethality were recorded.

The spore suspension of the target strain was inoculated in a 250 mL conical flask containing 30 mL of seed medium and incubated at 28 °C with rotary shaking at 200 rpm for 24 h. After incubation, 10 mL of the culture was collected, and the mycelia were harvested by centrifugation. The mycelia were washed twice with 5 mL of PB hypertonic solution (containing 2 mL trace element solution, 0.25 $g{\cdot}L^{-1}$ K_2SO_4, 120 $g{\cdot}L^{-1}$ sucrose, 2 $g{\cdot}L^{-1}$ $MgCl_2{\cdot}6\ H_2O$, and 10 mL of sterile $CaCl_2$ and 100 mL sterile KH_2PO_4, sterilized at 115 °C for 15 min). The washed mycelia were then resuspended in 5 mL of hypertonic PB solution, and 1 mL of lysozyme was added to digest the cell walls at 28 °C with continuous shaking (200 rpm) for 60 min to generate protoplasts.

For protoplast fusion, one parental strain was inactivated by UV treatment (15 W for 120 s), and the other by heat treatment (70 °C for 30 min). The detailed inactivation procedure is shown in Fig. S1a and S1b. Equal volumes (5 mL) of protoplast suspensions from each parental strain were mixed in a sterile centrifuge tube and centrifuged at 4000 rpm for 8 min to collect the protoplasts. The protoplasts were resuspended in 500 µL of sterile water, followed by the addition of 3 mL PEG solution, which was gently mixed by pipetting for 3 min. The mixture was incubated in a water bath at 25 °C for 20 min to promote the protoplast fusion. Subsequently, 4 mL of the PB solution was added, and the solution was homogenized by gentle pipetting. Finally, 100–300 µL of the fused protoplast solution was spread on regeneration medium and incubated at 28 °C.

Extraction of total RNA and quantitative real-time PCR (qRT-PCR)

Total RNA was extracted using TRIzol reagent (Shanghai Sangong Biotechnology Co., Ltd., China). cDNA synthesis was carried out using the HiScript III RT SuperMix for qPCR (+gDNA Wiper) kit (Vazyme, China) according to the manufacturer's protocol. Gene-specific primers for the target genes were designed using Beacon Designer 7 software. qRT-PCR was performed on a StepOne Real-Time PCR System (Applied Biosystems) using SYBR Premix Ex Taq (Takara, Japan). PCR conditions included an initial denaturation at 95 °C for 30 s, followed by 40 cycles of 10 s at 95 °C and 30 s at 60 °C. Each reaction was performed in a 20 µL system containing 10 µL of 2× ChamQ Universal SYBR qPCR Master Mix, 2 µL of DNA/cDNA template, 0.4 µL of forward and reverse primers (10 µM each), and 7.2 µL of ddH_2O. Relative transcript levels were quantified using the $2^{-\Delta\Delta Ct}$ method with 16 S as the internal reference gene [22]. The control transcript level was set to one, and the results were expressed as fold-changes relative to the control. Primer sequences for the target genes are listed in Table S2.

Sample preparation and transcriptome data processing

S. gilvosporeus ATCC13326 was cultured in a liquid fermentation medium, and 20 mL of the fermentation broth was collected after 72 h, based on the growth curve. The broth was centrifuged at 2960 × g for 25 min at 4 °C, and the pellet was retained. The pellet was washed three times with 20 mL of PBS, followed by another round of centrifugation to collect the bacterial cells, which were then rapidly frozen in liquid nitrogen. The samples were stored in liquid nitrogen and sent to Genedenovo (https://www.genedenovo.com/about/) for transcriptome sequencing. Data analysis and visualization were performed using the Omicsmart platform from GeneDenovo. Gene Ontology (GO) and Kyoto Encyclopedia of Genes and Genomes (KEGG) analyses were conducted using ClusterProfiler software. The de novo natamycin biosynthesis pathway was constructed based on the whole-genome data of *S. gilvosporeus* F607 (GenBank: CP020569.1). Pathways related to carbon metabolism, nitrogen metabolism, and branched-chain amino acid metabolism were constructed using KEGG database tools. The natamycin biosynthesis pathway was reconstructed based on experimentally validated findings [15]. The regulatory roles of PhoP and PhoR in natamycin biosynthesis were integrated based on the experimental results obtained in this study. Transcriptome data can be found at this link http://www.ncbi.nlm.nih.gov/bioproject/1179673.

Analysis methods

Natamycin concentration was measured using an Agilent 1260 Infinity II HPLC system (Agilent Technologies, USA) with a C18 reverse phase column (10 µL, 250 × 4.6 mm). For sample preparation, 1 mL of fermentation broth was mixed with 9 mL of extraction solution (methanol containing 5% acetic acid) and vortexed for 2 min. The mixture was centrifuged at 2960 × g for 25 min at 4 °C, and the supernatant was filtered through a 0.22 µm organic filter for HPLC analysis. The mobile phase was a water/methanol mixture (35:65, V/V), with a flow rate of 1 $mL{\cdot}min^{-1}$, a detection wavelength of 303 nm, and an injection volume of 10 µL [23]. The dry cell weight (DCW) of *S. gilvosporeus* strains was determined using the gravimetric method. Briefly, 4 mL of fermentation broth was centrifuged at 11,400 × g for 10 min, and the resulting pellet was dried at 105 °C to a constant weight. The residual glucose concentration was determined using a Biosensor Centrifuge 5804R (Shandong Academy of Sciences, China).

Data analysis

All experiments were performed in triplicate, and the resulting data are presented as mean ± standard deviation. Statistical analysis was conducted using the SPSS (version 22.0, SPSS Inc., Chicago, ILL, USA) through one-way analysis of variance (ANOVA) followed by Tukey's test ($p < 0.05$) for comparisons.

Results

Protoplast fusion combined with KH_2PO_4 tolerance screening enhances natamycin production

Firstly, the original strain S. gilvosporeus ATCC13326 was subjected to ARTP and DES mutagenesis to generate a mutant library with improved phosphate tolerance and increased natamycin production. The effects of different doses of ARTP (0–120 s), EMS (0–40 min), and KH_2PO_4 (0–5.6 $g{\cdot}L^{-1}$) on ATCC13326 cell death were investigated. The results showed that the optimal ARTP and EMS mutagenesis doses were 90 s and 30 min, respectively (Fig. S2a and S2b), with the initial screening concentration of phosphate set at 1.6 $g{\cdot}L^{-1}$ (Fig. S3).

After treatment with ARTP, the ATCC13326 spore suspension was spread on MS agar medium containing 1.6 $g{\cdot}L^{-1}$ KH_2PO_4 and incubated for 8–10 days. One hundred fast-growing mutants were randomly selected, and their production was evaluated using the agar cylinder method (Fig. 1a). Six mutant strains with the highest production were selected for shake flask fermentation, among which AP-1 had the highest production of 1.13 ± 0.06 $g{\cdot}L^{-1}$. Using AP-1 as the starting strain, two additional rounds of ARTP mutagenesis combined with phosphate tolerance screening, were conducted. Finally, a high-yielding mutant, AP-3, was obtained from 300 mutants, achieving a production of 1.45 ± 0.04 $g{\cdot}L^{-1}$ in shake flask fermentation, which was 1.81 times that of the original strain (Fig. 1d and e). Similarly, a mutant library

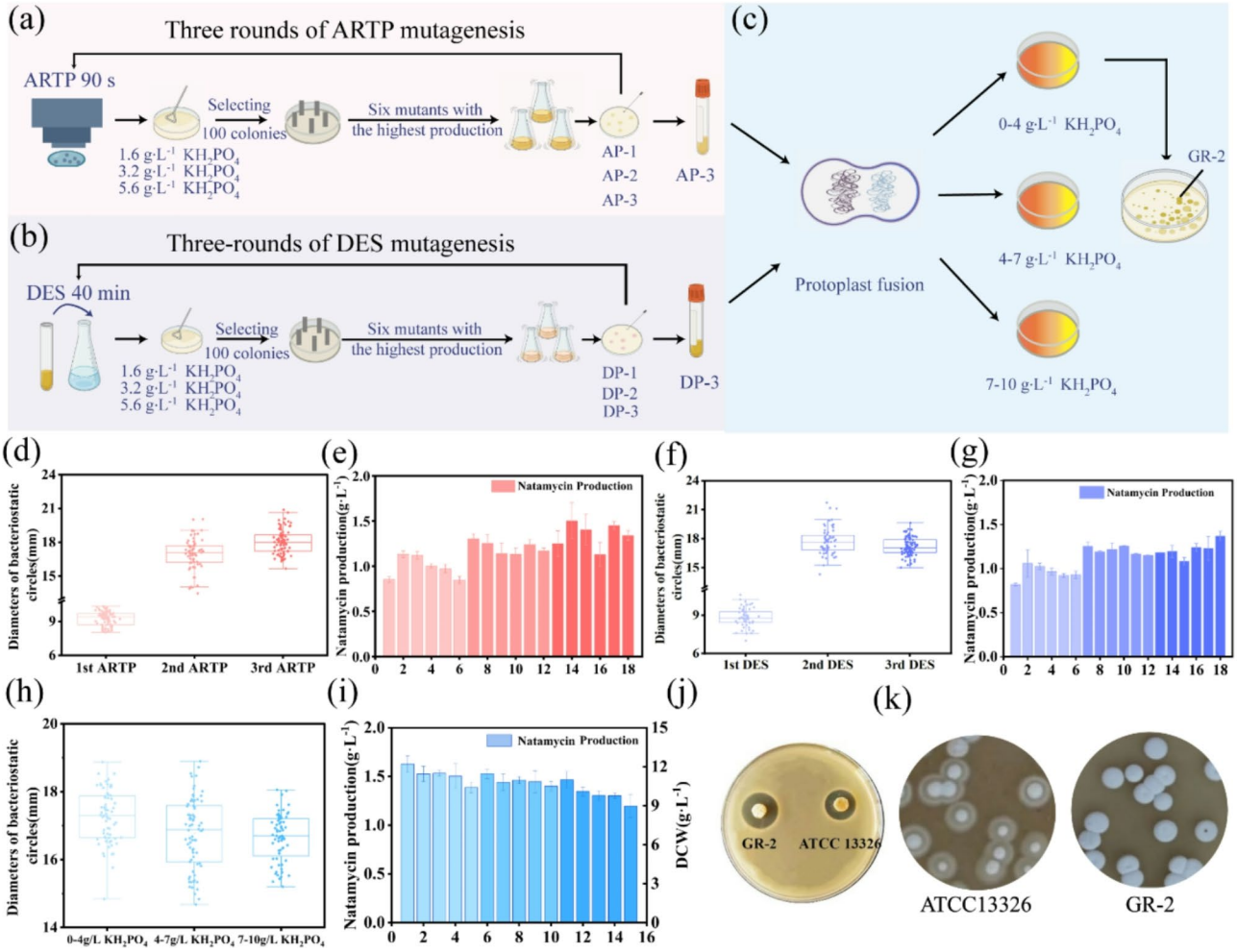

Fig. 1 Enhancing the natamycin production by protoplast fusion combined with KH_2PO_4 tolerance screening. **(a)** Flow diagrams of ARTP mutagenesis. **(b)** Flow diagrams of DES mutagenesis. **(c)** Flow diagrams of protoplast fusion. **(d)** and **(e)** Results of three rounds of ARTP mutagenesis. **(f)** and **(g)** Results of three rounds of DES mutagenesis. **(h)** and **(i)** Results of protoplast fusion. **(j)** and **(k)** Differences in natamycin production and mycelial growth between *S. gilvosporeus* ATCC13326 and *S. gilvosporeus* GR-2. DCW, cell dry weight. The error bars represent the standard error of the mean

was constructed by DES mutagenesis using ATCC13326 as the starting strain (Fig. 1b). After three rounds of DES mutagenesis combined with phosphate tolerance screening, the high-yielding strain DP-3 was obtained with a natamycin production of 1.36 ± 0.05 g·L^{-1}, 70% higher than that of ATCC13326 (Fig. 1f and g). These results indicate that ARTP and DES mutagenesis combined with phosphate tolerance screening can effectively increase natamycin production.

Compared with observations in DP-3, AP-3 exhibited higher natamycin production capacity but weaker mycelial growth capability (data not shown). Therefore, AP-3 and DP-3 were selected as the parental strains for protoplast fusion to obtain a high natamycin-yielding strain with improved spore growth. As shown in Figs. 1c and 300 protoplast fusion strains were obtained from plates with phosphate concentration gradients of 0 to 4 g·L^{-1}, 4 to 7 g·L^{-1}, and 7 to 10 g·L^{-1}. The production assessment results revealed that the mutants obtained from the 0–4 g·L^{-1} KH_2PO_4-resistant plates exhibited higher natamycin production. Among them, mutant GR-2 had the highest production, reaching 1.62 ± 0.03 g·L^{-1} inshake flask fermentation (Fig. 1h and i). Additionally, compared with observations in ATCC13326, the high-yielding strain GR-2 formed larger colonies and had stronger mycelial growth capacity (Fig. 1j and k). In summary, we developed a novel breeding method combining protoplast fusion with phosphate tolerance screening, which significantly increased natamycin production.

Differences in shake flask fermentation kinetics between the original strain ATCC1336 and the high-yielding mutant GR-2

To investigate the physiological changes in the high-yielding strain GR-2, a comparative analysis of the fermentation kinetics of ATCC1336 and GR-2 was conducted under the same cultivation conditions. During the first 24 h of fermentation, no significant differences were observed between ATCC1336 and GR-2 in glucose consumption rate, pH variation trends, biomass growth, or natamycin production rate (Fig. 2a and d). After 48 h, GR-2 exhibited a faster average glucose consumption rate, accelerated DCW increase, and rapid production of natamycin, indicating that this phase is the main stage for natamycin production. At 96 h, the DCW and natamycin production of GR-2 reached 14.12 ± 0.05 g·L^{-1} and 1.62 ± 0.03 g·L^{-1}, respectively, 77.5% and 102.5% higher compared with that of the original strain (Fig. 2a

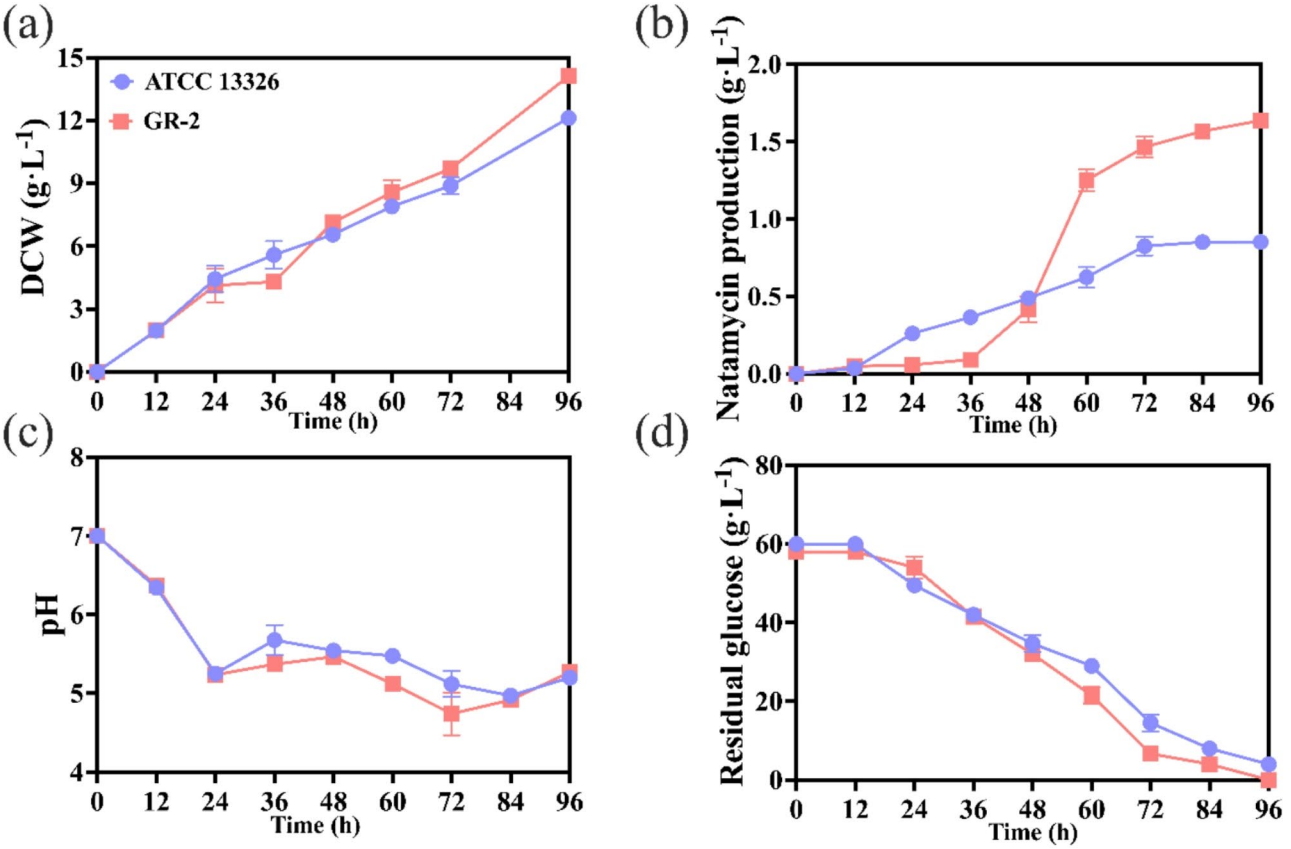

Fig. 2 Fermentation kinetics of the original strain *S. gilvosporeus* ATCC 13,326 and the high-yielding strain *S. gilvosporeus* GR-2. **(a)** Natamycin production. **(b)** Cell dry weight (DCW). **(c)** pH. **(d)** Residual glucose. The error bars represent the standard error of the mean

and b). These results demonstrated significant metabolic differences between the two strains. Since fermentation kinetics analysis cannot reveal the underlying factors contributing to high natamycin production, it is necessary to explore the intrinsic regulatory mechanisms of high GR-2 production through global transcriptional analysis. This will help identify the key metabolic pathways and nodes involved in natamycin biosynthesis, providing a theoretical foundation for further metabolic engineering modifications.

Analysis of the high-yielding mechanism of GR-2 based on transcriptomics

Global transcriptomic differences

Based on the fermentation kinetics curve, transcriptome of the original strain ATCC13326 and the high-yielding strain GR-2 was sampled at 72 h. The results showed that there were 1,246 differentially expressed genes (DEGs) between the two strains, of which 574 were upregulated and 672 were downregulated. GO analysis indicated that the upregulated DEGs were primarily enriched in membrane components, transport activity, and nucleic acid metabolism, whereas the downregulated DEGs were enriched in macromolecular biosynthesis and energy metabolism (Fig. S4a and S4b). KEGG enrichment analysis revealed that the DEGs were mainly enriched in branched-chain amino acids (BCAAs), carbohydrates, energy, and nucleotide metabolism (Fig. S4c).

The de novo natamycin biosynthetic pathway was constructed using genomic data from *S. gilvosporeus* F607 (GenBank: CP020569.1). As shown in Fig. 3, natamycin biosynthesis originates from acetyl-CoA and malonyl-CoA and is catalyzed by enzymes encoded by the natamycin BGC, a process that requires substantial consumption of NADPH [24–26]. By integrating the natamycin biosynthesis pathway with the results of the KEGG and GO enrichment analyses, the differences in carbohydrate metabolism, BCAA metabolism, nitrogen metabolism, and phosphate metabolism between GR-2 and the original strain ATCC13326 were analyzed to further explore the intrinsic mechanism underlying the high production of GR-2.

Carbohydrate metabolism

The glycolytic pathway is a key metabolic route in microorganisms that provides energy to cells and carbon skeletons for most biosynthetic products [27]. In the high-yielding GR-2 strain, the transcript levels of key enzymes of the glycolytic pathway, including fructose-1,6-bisphosphate aldolase (encoded by *fbaA*),

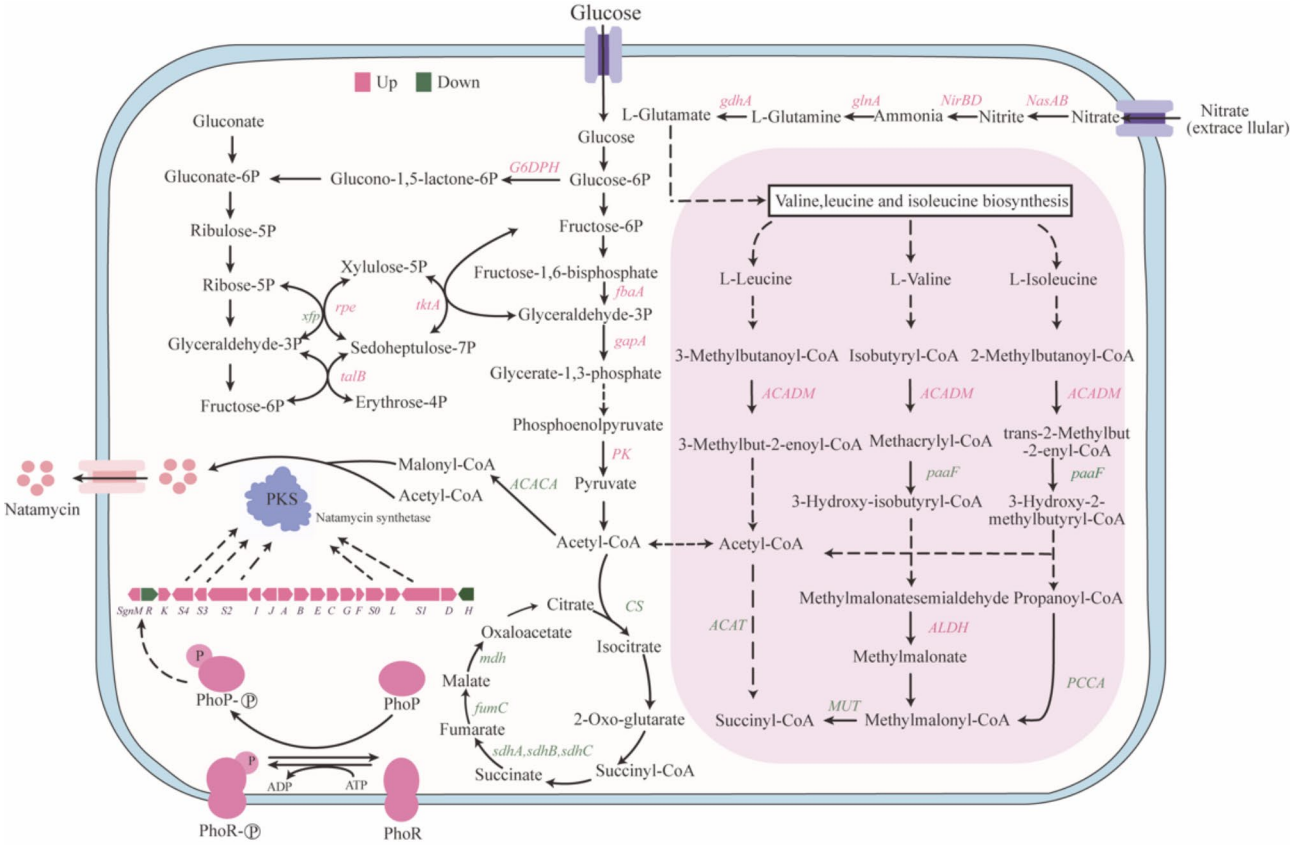

Fig. 3 The proposed mechanism for high natamycin production in *S. gilvosporeus* GR-2

Table 1 Differentially expressed genes in the glycolytic pathway

Gene	Gene ID	Description	Log_2 (FC) (GR /WT)
DLAT	B1H19_RS03740	2-oxo acid dehydrogenase subunit E2	-2.06
ALDH	B1H19_RS09065	aldehyde dehydrogenase family protein	1.11
PK	B1H19_RS11960	pyruvate kinase	1.45
aceE	B1H19_RS12835	pyruvate dehydrogenase (acetyl-transferring), homodimeric type	-1.13
ppdK	B1H19_RS14515	pyruvate, phosphate dikinase	-2.63
yahK	B1H19_RS22385	NAD(P)-dependent alcohol dehydrogenase	1.05
ALDH	B1H19_RS23330	aldehyde dehydrogenase family protein	2.40
pckA	B1H19_RS26025	phosphoenolpyruvate carboxykinase (GTP)	-1.10
PK	B1H19_RS27770	pyruvate kinase	-1.03
gapA	B1H19_RS30875	glyceraldehyde-3-phosphate dehydrogenase	1.61
fbaA	B1H19_RS34160	class II fructose-bisphosphate aldolase family protein	1.62

Table 2 Differentially expressed genes in the branched-chain amino acid metabolism

Gene	Gene ID	Description	Log_2 (FC) (GR /WT)
ALDH	B1H19_RS09065	Aldehyde dehydrogenase family protein	2.40
acd	B1H19_RS09080	Acyl-CoA dehydrogenase	1.21
MUT	B1H19_RS25485	Methylmalonyl-CoA mutase family protein	-2.29
ACAT	B1H19_RS34225	Acetyl-CoA C-acetyltransferase	-1.29

glyceraldehyde-3-phosphate dehydrogenase (encoded by *gapA*), and pyruvate kinase (encoded by *PK*), were upregulated 3.07-fold, 3.05-fold, and 2.73-fold, respectively (Table 1). Fructose-1,6-bisphosphate aldolase catalyzes its cleavage to form glyceraldehyde-3-phosphate, whereas pyruvate kinase catalyzes the conversion of phosphoenolpyruvate to pyruvate. Increased transcription of these enzymes promotes pyruvate production, leading to increased acetyl-CoA synthesis. This may be one of the reasons for the increased natamycin production in GR-2. The TCA cycle plays a crucial role in supplying energy, synthesizing intermediate metabolites, and balancing the conversion of carbohydrates, fats, and proteins [28]. Compared to observations in the ATCC1336 strain, 12 DEGs in the TCA cycle were significantly downregulated in GR-2. Citrate synthase, the first key enzyme in the TCA cycle, exhibited a 2.14-fold decrease in transcript levels, resulting in reduced isocitrate synthesis. Additionally, the transcript levels of succinate dehydrogenase (encoded by *sdhA, sdhB*, and *sdhC*), fumarate hydratase (encoded by *fumC*), and malate dehydrogenase (encoded by *mdh*) were significantly downregulated, which further weakened the TCA cycle (Table S3).

The pentose phosphate pathway (PPP) is the primary route for NADPH production [29]. In GR-2, the transcription levels of ribose-5-phosphate isomerase (encoded by *RPE*), transketolase (encoded by *tktA*), transaldolase (encoded by *talB*), and glucose-6-phosphate dehydrogenase (encoded by *G6PDH*) in the PPP pathway were all upregulated. Glucose-6-phosphate dehydrogenase is the first key enzyme in the PPP, catalyzing the conversion of glucose-6-phosphate to 6-phosphogluconate, while reducing $NADP^+$ to NADPH, thus providing reducing power to the cell. Although transketolase, transaldolase, and glucose-6-phosphate dehydrogenase are not directly involved in NADPH biosynthesis, they maintain the balance of the PPP, by indirectly promoting NADPH production [30].

In summary, the significant upregulation of the glycolysis pathway and downregulation of the TCA cycle in GR-2 promoted the production of acetyl-CoA. PPP upregulation provides sufficient reducing power (NADPH) for natamycin synthesis. These factors may explain the significantly increased natamycin biosynthesis efficiency in GR-2.

BCAA degradation pathway

BCAAs, such as leucine, isoleucine, and valine, play important metabolic and physiological roles in microorganisms [31]. The degradation pathways of BCAAs provide two- and three-carbon compounds, such as acetyl-CoA and propionyl-CoA, to microbial cells. Four DEGs were found to be involved in the BCAA degradation pathway in GR-2 (Table 2). Among them, acyl-CoA dehydrogenase (encoded by *acd*) and acetaldehyde dehydrogenase (encoded by *ALDH*) were upregulated 2.17-fold and 4.72-fold, respectively, promoting the synthesis of acetyl-CoA and malonyl-CoA. Transcription of methylmalonate transferase was downregulated 4.89-fold, increasing the availability of methylmalonic acid and promoting the production of methylmalonyl-CoA. These changes indicate that the enhanced BCAA catabolic pathway in GR-2 is conducive to generating the precursors required for natamycin synthesis, which may further enhance natamycin production.

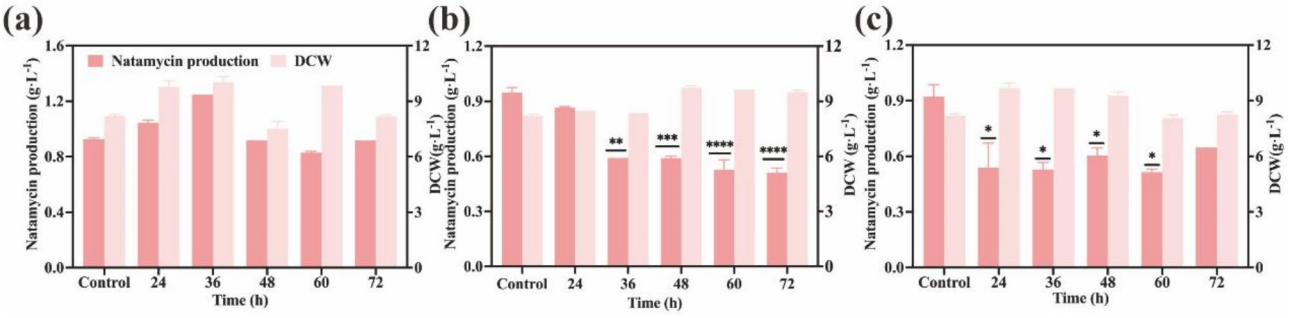

Fig. 4 Effects of exogenously addition of branched-chain amino acids at different time points on natamycin production of *S. gilvosporeus* ATCC 13,326. **(a)** Valine; **(b)** Leucine; **(c)** Isoleucine. The error bars represent the standard error of the mean. Asterisk denotes statistically significant differences: *$p < 0.05$; **$p < 0.01$; ***$p < 0.001$; ****$p < 0.001$

Table 3 Differentially expressed genes in the nitrogen metabolism

Gene	Gene ID	Description	Log_2 (FC) (GR /WT)
gltD	B1H19_RS12025	Glutamate synthase subunit beta	-1.98
gltB	B1H19_RS12030	Glutamate synthase large subunit	-1.8
glnA	B1H19_RS12950	Glutamine synthetase beta-grasp domain-containing protein	1.46
gdhA	B1H19_RS28090	NADP-specific glutamate dehydrogenase	1.67
nirB	B1H19_RS14410	Nitrite reductase large subunit NirB	1.55
nasB	B1H19_RS14405	FAD-dependent oxidoreductase	1.27
nasA	B1H19_RS14320	Molybdopterin Oxidoreductase family protein	2.06
cynT	B1H19_RS05995	Carbonic anhydrase	-1.14
nirD	B1H19_RS14415	nitrite reductase small subunit NirD	1.51

To investigate the effect of BCAAs on natamycin synthesis, BCAA feeding experiments were conducted using ATCC13326 in shake flasks. During fermentation, valine was added to the culture medium at 24, 36, 48, 60, and 72 h at a final concentration of 0.50 g·L^{-1}. The results showed that the addition of valine at the early phases of fermentation (24 and 36 h) significantly increased natamycin production, especially at 36 h, when natamycin production reached 1.21 ± 0.06 g·L^{-1}, a 50% increase compared to that of the control (Fig. 4a). However, valine addition during the middle and late phases of fermentation (48, 60, and 72 h) had no significant effect on natamycin production. This may be due to an insufficient intracellular supply of valine in the ATCC13326 strain during the early phases of fermentation (Fig. S5). The addition of leucine or isoleucine did not significantly promote natamycin production (Fig. 4b and c). In summary, the enhancement of intracellular valine degradation pathway in GR-2 cells is a key factor for high natamycin production.

Nitrogen metabolism

In GR-2, seven DEGs involved in nitrogen metabolism were identified, of which six were upregulated and one was downregulated (Table 3). Nitrate and nitrite reductase are two key enzymes in the nitrate assimilation system and are primarily involved in nitrogen uptake and utilization by microorganisms [32]. Upregulation of their transcription increases the efficiency of nitrogen utilization by providing more precursors for the synthesis of glutamate and glutamine. The transcript levels of glutamate dehydrogenase (encoded by *gdhA*) and glutamine synthetase (encoded by *glnA*) increased by 3.18-fold and 2.75-fold, respectively, further enhancing the synthesis of glutamate and glutamine. However, the glutamate content of GR-2 was lower than that of ATCC13326 (data not shown). These results indicated that the supply of glutamate in GR-2 was insufficient, resulting in a nitrogen-limited state. By transcriptionally activating nitrogen metabolism, the cells increase glutamate and glutamine synthesis, thereby indirectly promoting natamycin synthesis. The effects of glutamate and glutamine on natamycin production were further investigated using amino acid addition experiments. The results showed that the addition of glutamate at 36 h and glutamine at 60 h significantly increased natamycin production (Fig. 5a and b).

To further verify the effect of upregulated nitrogen metabolism on natamycin synthesis, the *nasA*, *nasB*, *gdhA*, and *nirB* genes from *S. gilvosporeus* ATCC13326 were amplified and ligated into the pIB139 vector, to construct the pIB139-*nasA*, pIB139-*nasB*, pIB139-*gdhA*, and pIB139- *nirB* expression vectors. These genes were overexpressed under the control of the *ermEp* promoter from *Saccharopolyspora erythraea* and introduced into *S. gilvosporeus* via conjugation, resulting in engineered strains

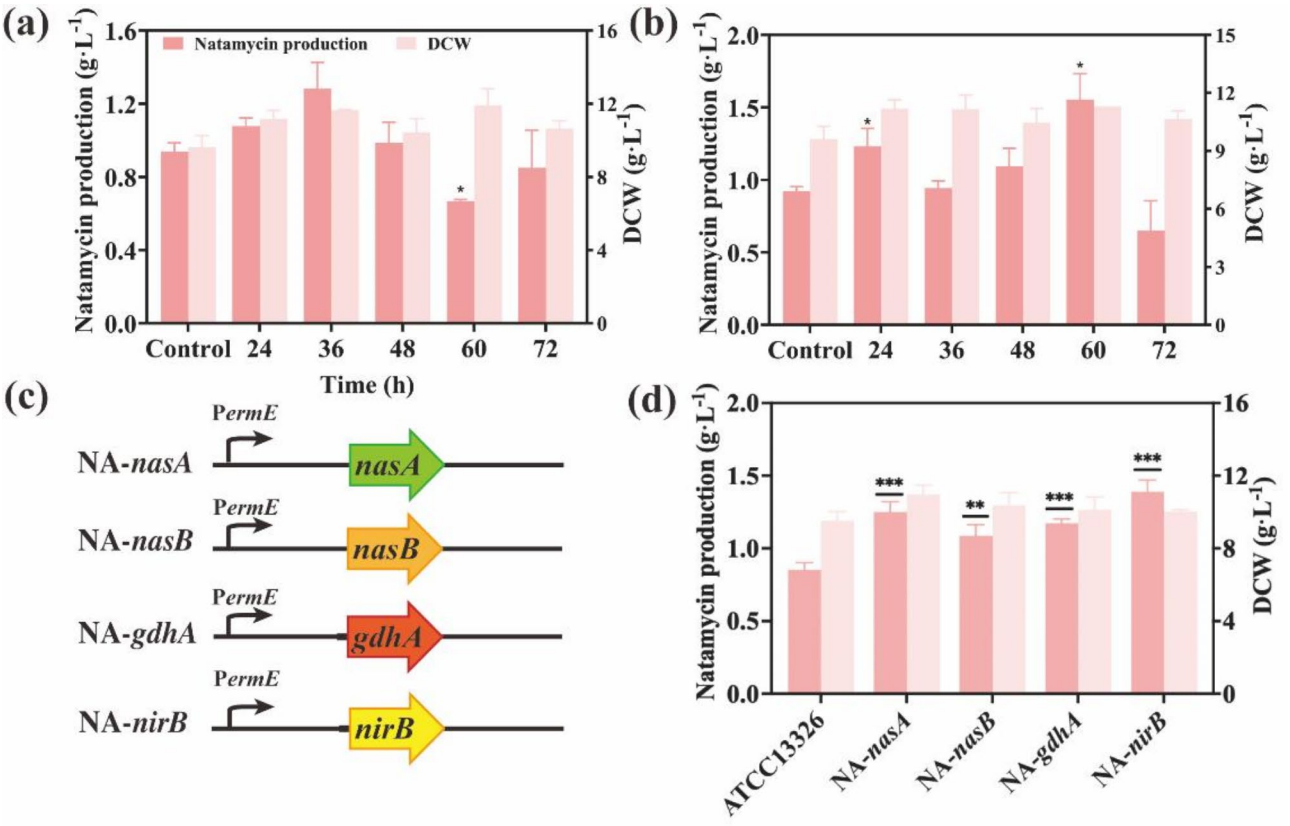

Fig. 5 Effect of nitrogen metabolism on natamycin production of *S. gilvosporeus* ATCC 13,326. **(a)** Adding exogenously glutamate enhances the natamycin production. **(b)** Adding exogenously glutamine enhances the natamycin production. **(c)** Schematic of the construction of strains. **(d)** Overexpressing *nasA, nasB, gdhA,* and *nirB* enhances the natamycin production. The error bars represent the standard error of the mean. Asterisk denotes statistically significant differences: *$p < 0.05$; **$p < 0.01$; ***$p < 0.001$

NA-*nasA*, NA-*nasB*, NA-*gdhA*, and NA-*nirB* (Fig. 5c). Shake flask fermentation results showed that the overexpression of *gdhA*, *nasA*, *nasB* and *nirB* significantly enhanced natamycin synthesis (Fig. 5d).

In summary, the improvement of nitrogen metabolism significantly increased the synthesis of glutamate and glutamine, which effectively promoted natamycin biosynthesis in GR-2.

Phosphate metabolism

Because the highly productive mutant GR-2 was obtained through phosphate tolerance screening, the transcription of genes related to intracellular phosphate metabolism may have changed. KEGG analysis of phosphate metabolism-related DEGs revealed that the transcript levels of the phosphate-responsive two-component system (TCS) PhoR (response regulator) and PhoP (sensor protein), as well as PhoU (regulator of PhoR/PhoP) were upregulated in GR-2 (Table S4) [33–34]. It has been reported that at low phosphate concentrations, PhoR activates PhoP via phosphorylation, thereby regulating the transcription of genes involved in phosphate metabolism. This helps to balance intracellular phosphate levels and enhances the phosphate adaptability of cells [35]. PhoR-PhoP can regulate the synthesis of secondary metabolites, such as daptomycin and erythromycin [36, 37]. Therefore, the upregulation of PhoR and PhoP in GR-2 may be one of the reasons for the increased natamycin production. To study the impact of PhoR and PhoP on natamycin synthesis, strains NA-*phoR* and NA-*phoP* were constructed, in which *phoR* and *phoP* were overexpressed under the control of a strong promoter P*ermE** (Fig. 6a). The natamycin productions of NA-*phoR* and NA-*phoP* were 1.21 ± 0.04 g·L^{-1} and 1.32 ± 0.05 g·L^{-1}, respectively, 51.2% and 65.0% higher than that of ATCC13326 (Fig. 6b). Subsequently, Sg-anti*phoR* and Sg-anti*phoP* strains were constructed in which the translation of PhoR and PhoP mRNAs was inhibited using antisense RNAs of these genes under the control of P*ermE**. Natamycin production by Sg-anti*phoR* and Sg-anti*phoP* was significantly lower than that of ATCC13326 (Fig. 6c). In Sg-anti*phoR* and Sg-anti*phoP*, most of the genes involved in natamycin BGC were significantly downregulated (Fig. 6d), suggesting that PhoR and PhoP may regulate the synthesis of natamycin by regulating the expression of genes in BGC. Furthermore, the overexpression of PhoR and PhoP

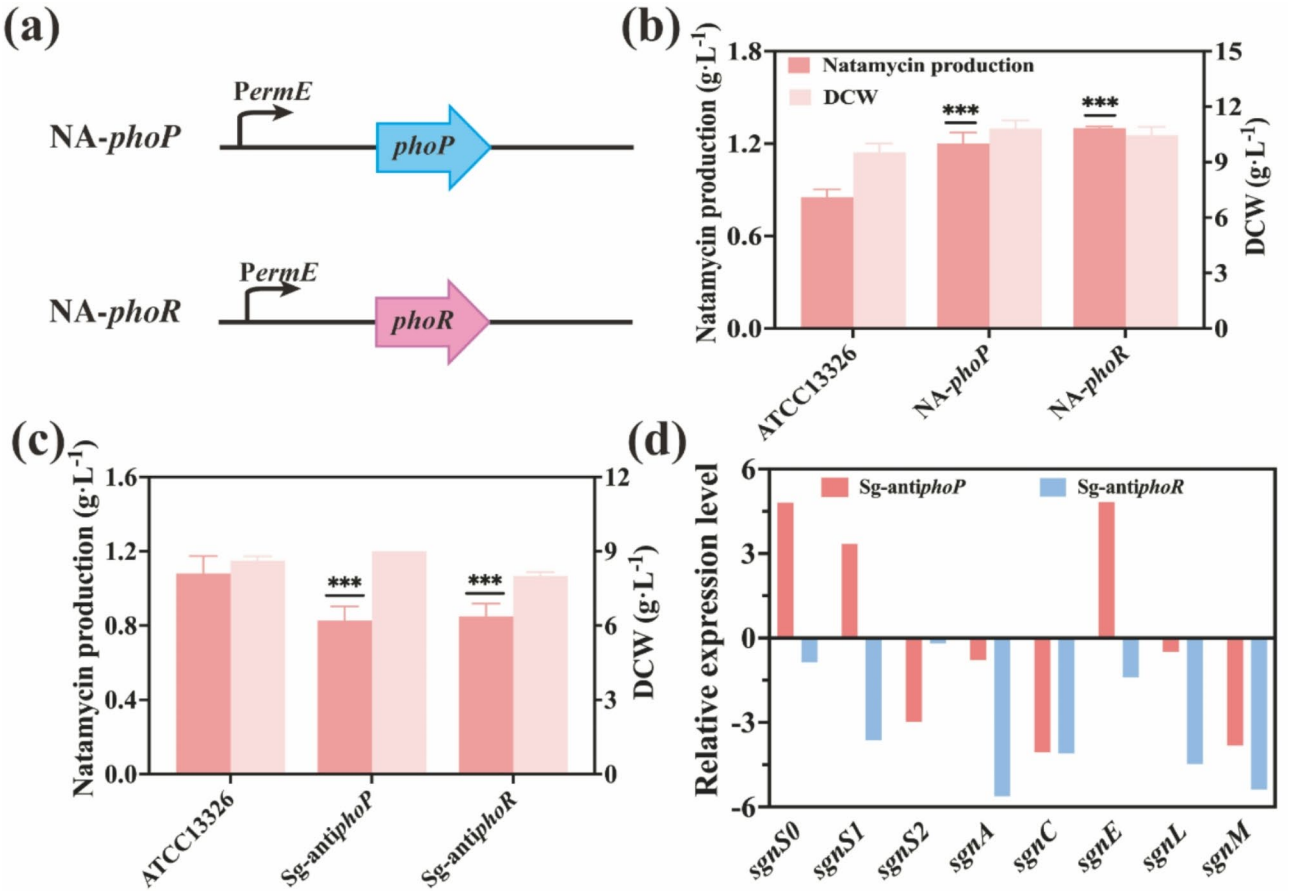

Fig. 6 Effect of phosphate metabolism on natamycin production of *S. gilvosporeus* ATCC 13,326. **(a)** Schematic of the construction of strains. **(b)** Overexpressed *phoP* or *phoR* enhances the natamycin production. **(c)** Silenced *phoP* and *phoR* decreases the natamycin production. **(d)** Silenced *phoP* or *phoR* represses the expression of natamycin biosynthetic gene cluster. The error bars represent the standard error of the mean. Asterisk denotes statistically significant differences: *** $p < 0.001$

promoted cell growth, whereas inhibition of their expression led to a decrease in biomass. These results indicate that PhoR/PhoP may be involved in both natamycin biosynthesis and physiology of *S. gilvosporeus*. In summary, phosphate tolerance screening may have activated the expression of the PhoR/PhoP TCS system, thereby increasing natamycin production in GR-2.

Natamycin biosynthesis pathway

Natamycin is synthesized by the natamycin BGC, which includes 19 genes from *sgnS0* to *sgnM* (Table 4) [24]. In the GR-2 cells, 16 DEGs involved in the BCG were upregulated. Among them, genes encoding polyketide synthases (*sgnS0* to *sgnS4)* were upregulated 2.86 to 3.83-fold. Genes encoding proteins responsible for carbon skeleton modification (*sgnC, sgnD, sgnE, sgnG, sgnJ*, and *sgnK*) and natamycin transporters (*sgnA* and *sgnB*) were also significantly upregulated by 1.45 to 13.08-fold. High expression of natamycin biosynthesis genes, such as *sgnE* and *sgnJ*, can directly promote its production. Therefore, the upregulated transcript levels of genes involved in the BGC are an important reason for the high natamycin production in GR-2. The transcriptome data were further validated by qRT-PCR, and the results showed that the transcription levels of the 19 genes involved in the BGC were generally consistent with the transcriptome results, suggesting that the transcriptome data were reliable (Fig. S6).

Possible mechanisms underlying high natamycin production in GR-2

Based on the above results, the high production mechanism of the GR-2 strain was suggested (Fig. 3): the upregulated glycolytic pathway and the downregulated TCA cycle promote the production of intracellular acetyl-CoA in GR-2. The significantly upregulated nitrogen metabolism pathway enhances the uptake of nitrogen sources and the biosynthesis of glutamate and glutamine in GR-2. The increased supply of glutamate and glutamine, together with the upregulated BCAA catabolic pathway, jointly promotes the generation of acetyl-CoA and malonyl-CoA. Additionally, upregulation of the pentose

Table 4 Differentially expressed genes in the natamycin biosynthetic gene cluster [24]

Gene	Gene ID	Description	Log2 (FC) (GR /WT)
sgnS0	B1H19_RS05075	Type I polyketide synthase	1.52
sgnS1	B1H19_RS05085	Type I polyketide synthase	2.72
sgnS2	B1H19_RS05030	Type I polyketide synthase	1.92
sgnS3	B1H19_RS05020	Type I polyketide synthase	1.94
sgnS4	B1H19_RS05020	Type I polyketide synthase	1.94
SgnA	B1H19_RS05045	ABC transporter ATP-binding protein	3.24
sgnB	B1H19_RS05050	ABC transporter ATP-binding protein	3.40
sgnC	B1H19_RS05060	DegT/DnrJ/EryC1/StrS family aminotransferase	1.33
sgnD	B1H19_RS05090	Cytochrome P450	2.15
sgnE	B1H19_RS05055	GMC oxidoreductase	1.61
sgnF	B1H19_RS05070	Ferredoxin	1.05
sgnG	B1H19_RS05065	Cytochrome P450	1.07
sgnI	B1H19_RS05035	Alpha/beta fold hydrolase	2.83
sgnJ	B1H19_RS05040	GDP-mannose 4,6-dehydratase	3.71
sgnK	B1H19_RS05015	Glycosyltransferase	1.89
sgnL	B1H19_RS05080	Tyrosine-protein phosphatase	1.31
sgnM	B1H19_RS05005	LuxR C-terminal-related transcriptional regulator	0.54
sgnR	B1H19_RS05010	AfsR/SARP family transcriptional regulator	-0.44
sgnH	B1H19_RS05145	MFS transporter	-1.76

pathway provides more NADPH for natamycin and intracellular amino acid synthesis. The natamycin synthesis gene cluster was significantly upregulated. These factors synergistically facilitate the efficient biosynthesis of natamycin in GR-2.

Reinforced phosphate metabolism promotes natamycin synthesis

Physiological and transcriptomic results indicated that enhancing phosphate metabolism can promote natamycin production. To further increase natamycin production, we enhanced phosphate metabolism in GR-2 cells by overexpressing *phoR* and *phoP*. The following strains were constructed: recombinant strain GR2-P1 for overexpressing *phoR* in GR-2, recombinant strain GR2-P2 for overexpressing *phoP* in GR-2, and recombinant strain GR2-P3 for co-overexpressing *phoP* and *phoR* in GR-2 (Fig. 7a). The natamycin production of GR-P1 and GR-P2 was 1.77 ± 0.1 g·L^{-1} and 1.88 ± 0.1 g·L^{-1}, respectively, 7.93 and 14.63% higher than that of the host strain GR-2 (Fig. 7b). These results indicated that the improvement of phosphate metabolism could further enhance natamycin production in GR-2.

Finally, the fed-batch fermentation performance of the high-yielding engineered strain GR2-P3 was evaluated in a 5 L fermenter (Fig. 7c). As fermentation progressed, both the pH and DO levels decreased. When the pH dropped to 6.0, it was maintained at 6.0 by automatically adding 25% ammonia. When the DO dropped to 20%, it was maintained above 20% by adjusting the aeration and rotation speed. The results showed that the DCW increased rapidly to 15.6 g·L^{-1} before 48 h, and the growth rate slowed significantly after 72 h. Natamycin production began to increase from 24 h until the end of fermentation. Finally, after 120 h of fermentation, the DCW and natamycin production of GR2-P3 reached 28.73 g·L^{-1} and 12.2 g·L^{-1}, respectively (Fig. 7c).

Discussion

Natamycin, a natural secondary metabolite produced primarily by *S. gilvosporeus*, is widely used in food preservation, medicine, agriculture, and cosmetics. However, high production costs and low yields are the main bottlenecks limiting the industrial production of natamycin. To enhance natamycin production, protoplast fusion combined with phosphate tolerance screening was applied to obtain a high-yielding strain, GR-2. Through fermentation kinetics analysis, we found that the GR-2 exhibited high rates of glucose consumption, increased biomass, and natamycin synthesis in the late stages of fermentation. Comparative transcriptomic analysis was then conducted to investigate the differences in intracellular metabolism and natamycin biosynthesis between the high-yielding strain and the original strain ATCC13326, with the aim of providing rational guidance for natamycin synthesis. KEGG enrichment results showed a strong correlation between carbohydrate metabolism, nitrogen metabolism, BCAA metabolism, phosphate metabolism, and the high natamycin production of GR-2.

Analysis of carbohydrate metabolism indicated that the upregulation of the glycolytic pathway and downregulation of the TCA cycle in GR-2 were beneficial for the production of the natamycin precursor acetyl-CoA, thereby promoting natamycin biosynthesis. Similarly,

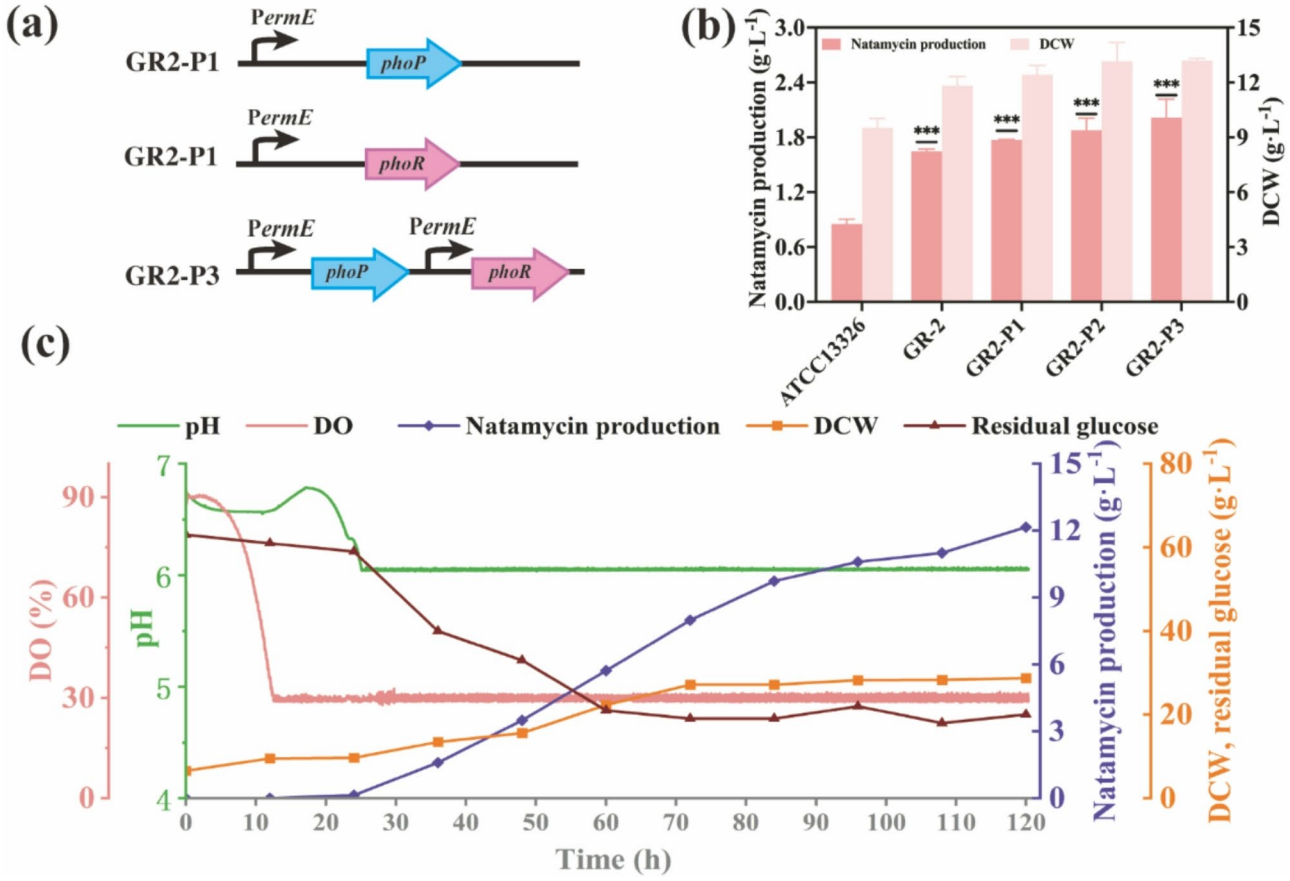

Fig. 7 Fermentation performances of *S. gilvosporeus* GR2-P3. **(a)** Schematic of the construction of strains. **(b)** Shake flask fermentation performances of ATCC 13,326, GR-2, GR2-P1, GR2-P2, and GR2-P3. The error bars represent the standard error of the mean. **(c)** Fed-batch fermentation performances of GR2-P3

Zhang et al. reported that mutations enhanced the glycolytic pathway, leading to the production of acetyl-CoA, which in turn increased amphotericin production [38]. Moreover, as a macrolide polyene antibiotic, natamycin biosynthesis requires a significant amount of NADPH for polyene polymerization and redox reactions. Therefore, the upregulation of the PPP pathway in GR-2 may facilitate natamycin synthesis by providing more NADPH. Enhancing the PPP pathway is crucial for the generation of NADPH and the production of secondary metabolites, such as 1,5-diaminopentane, 3-hydroxypropionic acid, actinorhodin, and bacitracin [39–42]. Therefore, utilizing metabolic engineering to enhance the glycolytic pathway and PPP in natamycin-producing strains while inhibiting the TCA cycle may be an important strategy to increase natamycin production.

Our study demonstrated that only the exogenous addition of valine during the early phases of fermentation significantly enhanced natamycin production, whereas the addition of the other two BCAAs did not have a similar effect. Valine is degraded to produce methylmalonyl-CoA, whereas leucine and isoleucine are degraded to acetyl-CoA. This suggests that the supply of methylmalonyl-CoA is insufficient in ATCC13326 cells, limiting natamycin biosynthesis. Bacitracin, a secondary metabolite produced by *Bacillus licheniformis*, shares the same precursors (acetyl-CoA and methylmalonyl-CoA) as natamycin. Enhancing the supply of BCAAs can significantly increase bacitracin production, which is consistent with our results [43, 44]. Therefore, synergistically enhancing valine biosynthesis and degradation or improving the methylmalonyl-CoA supply represents a potential strategy for improving natamycin production.

In addition, the effect of nitrogen metabolism on natamycin biosynthesis was identified and validated for the first time. Transcriptome analysis, overexpression, and exogenous amino acid feeding experiments demonstrated that the enhanced nitrogen metabolism in GR-2 increased the intracellular supply of glutamate and glutamine, ultimately promoting natamycin synthesis. Glutamate, as the primary amino acid donor in cells, contributes to increased BCAA availability, thereby enhancing natamycin production by GR-2 [45]. Glutamine can be transformed to glutamate by glutamine synthetase,

making it a major intracellular source of glutamate. Thus, glutamine may promote natamycin biosynthesis by providing glutamate to cells. Despite the importance of nitrogen metabolism in promoting natamycin synthesis, certain limitations remain. For instance, although overexpression of genes involved in nitrogen metabolism and the exogenous addition of glutamate and glutamine significantly increased natamycin production, the precise regulatory mechanisms underlying these effects have not yet been fully elucidated. Future research in this area will be of great significance.

Phosphate-tolerant strains exhibit enhanced environmental adaptability, which allows them to maintain high growth rates under adverse conditions through metabolic regulation [46]. Santos-Beneit et al. found that phosphate concentration strongly regulates vancomycin resistance in *Streptomyces coelicolor*, and this regulation is not mediated by PhoP. As the phosphate concentration increases, the vancomycin tolerance of *S. coelicolor* gradually decreases [47]. Further studies revealed that high phosphate concentrations inhibit the expression of vancomycin resistance genes, thereby reducing bacterial vancomycin resistance [48]. However, this mechanism is not sufficient to explain how phosphate tolerance promotes natamycin biosynthesis. Transcriptome analysis revealed that the selection for phosphate tolerance led to the upregulation of phosphate metabolism related proteins (PhoU) and transcriptional regulators (PhoP) in the GR-2 strain, promoting phosphate transport and uptake, resulting in enhanced cell growth. This may also be one of the reasons why the DCW of the GR-2 strain is significantly higher than that of ATCC13326.

Further research revealed that the TCS PhoP and PhoR act as positive regulators of the natamycin biosynthesis gene cluster (Fig. 6). Notably, in *Streptomyces natalensis*, the PhoP-PhoR deletion mutant exhibited overproduction of pimaricin (a synonym for natamycin), which seems to contradict our conclusion. This discrepancy may be attributed to the species-specific regulatory role of PhoP-PhoR in the biosynthesis of secondary metabolites in different *Streptomyces* species. In *S. coelicolor*, PhoP competitively binds to the *afsS* promoter, thereby inhibiting AfsR activation of *afsS*, leading to the downregulation of antibiotic biosynthesis. Meanwhile, AfsR can reverse regulate *phoR-phoP* and *pstS*, indicating the existence of a complex cross-regulation between PhoP and AfsR, which allows the strain to adapt to the phosphate availability and regulate secondary metabolic pathways [49]. Under phosphate-limiting conditions in *Streptomyces tsukubaensis*, PhoP enhances FK506 biosynthesis by regulating primary metabolism genes to increase precursor availability and upregulating *fkbN*, a key regulator of FK506 production [50]. In *Streptomyces lividans*, the PhoR-PhoP system not only directly affects phosphate metabolism but also negatively regulates secondary metabolite biosynthesis via phosphate signaling. PhoR-PhoP deletion mutants exhibited overproduction of actinorhodin and undecylprodigiosin under both low- and high-phosphate conditions, whereas the wild-type strain demonstrated phosphate-mediated negative regulation under high-phosphate environments [51]. These studies revealed the critical role of PhoP-PhoR in the regulation of natamycin biosynthesis and provide new insights into the molecular regulatory mechanisms of secondary metabolism in *Streptomyces*.

In this study, a novel method, protoplast fusion combined with phosphate tolerance screening, was used to enhance natamycin production in *S. gilvosporeus*, and the high-yield mechanism was elucidated through transcriptome analysis. Compared to the original strain ATCC13326, GR-2 showed (1) upregulation of the glycolysis pathway and downregulation of the TCA cycle, promoting the production of acetyl-CoA; (2) enhanced BCAA degradation pathway, particularly the valine degradation pathway, which increased the supply of methylmalonyl-CoA; (3) enhanced nitrogen metabolism, leading to an increased supply of glutamate and glutamine; and (4) upregulation of the PhoR-PhoP system, which improved phosphate metabolism and activated the expression of the BGC of natamycin. These metabolic changes are the main reasons for high natamycin production in GR-2. Based on these results, co-overexpression of *phoR* and *phoP* further increased natamycin production in GR-2. In a 5 L fermenter, the engineered strain achieved a natamycin production of 12.2 ± 0.61 g·L^{-1}, which is 52.5% higher than the original strain ATCC13326. This study provided an effective method to enhance natamycin production and identified key metabolic pathways and molecular targets influencing its biosynthesis, providing a theoretical basis for optimizing industrial production. The findings also offer insights that could be applied to the synthesis and regulation of other secondary metabolites. Future research should investigate the regulatory mechanisms of nitrogen and phosphate metabolism in natamycin biosynthesis and further optimize these pathways through metabolic engineering to enhance natamycin production.

Supplementary Information

The online version contains supplementary material available at https://doi.org/10.1186/s12934-025-02696-y.

Supplementary Material 1

Author contributions

LW: Investigation, Visualization, Writing original draft, Writing-review & editing. WX: Investigation, Writing - review & editing. TQ: Investigation. HZ: Investigation. JZ: Investigation. XC: Supervision, Funding acquisition. All authors read and approved the final manuscript.

Funding
This work was supported by the National Key R&D Program of China, 2020YFA0907700; Key R&D Program of Jiangsu Province, BE2022703; Jiangsu Agricultural Science And Technology Innovation Fund, CX(24)3086 L; The Fundamental Research Funds for the Central Universities (JUSRP123040); Program of the Key Laboratory of Industrial Biotechnology, Ministry of Education, China (KLIB-KF202206).

Data availability
No datasets were generated or analysed during the current study.

Declarations

Ethics approval and consent to participate
All authors read and approved the final manuscript and related ethics.

Consent for publication
All authors consent to this manuscript for publication after revising this final form.

Competing interests
The authors declare no competing interests.

Author details
[1]Key Laboratory of Industrial Biotechnology, School of Biotechnology, Ministry of Education, Jiangnan University, Wuxi 214122, China

Received: 2 November 2024 / Accepted: 13 March 2025
Published online: 02 April 2025

References

1. Zong GL, Wei L, Zhang J, Zhang J, Zhang B, Zhang L, et al. Novel mechanism of hydrogen peroxide for promoting efficient Natamycin synthesis in *Streptomyces Gilvosporeus* F607. Microbiol Spectr. 2023;11:e00879–23.
2. Khames A, Khaleel M, El-Badawy MF, El-Nezhawy AO. Natamycin solid lipid nanoparticles–sustained ocular delivery system of higher corneal penetration against deep fungal keratitis: Preparation and optimization. Int J Nanomed. 2019;14:2515–31.
3. Cao YX, Zhang X, Song X, Li W, Ren Z, Feng J, et al. Efficacy and toxic action of the natural product Natamycin against *Sclerotinia sclerotiorum*. Pest Manag Sci. 2024;80:1981–90.
4. Zeng X, Lin B, Luo J, Li W, Qi B, Wan Y, et al. Production of Natamycin by Z28 through solid-state fermentation using agro-industrial residues. Bioresour Technol. 2019;273:377–85.
5. Elsayed EA, Farid M, El-Enshasy H. Enhanced Natamycin production by *Streptomyces natalensis* in shake-flasks and stirred tank bioreactor under batch and fed-batch conditions. BMC Biotechnol. 2019;19:65.
6. Zeng X, Lin B, Wan Y, Li W, Luo J, Liang Z. Waste cooking oil: new efficient carbon source for Natamycin production by *Streptomyces Gilvosporeus* Z8. Process Biochem. 2022;118:294–306.
7. Shen WH, Wang DH, Wei LL, Zhang Y. Fungal elicitor-induced transcriptional changes of genes related to branched-chain amino acid metabolism in *Streptomyces natalensis* HW-2. Appl Microbiol Biotechnol. 2020;104:4471–82.
8. Ge J, Wang CL, Huang SF, Du R, Liu K, Song G, et al. Biosynthesis regulation of Natamycin production from *Streptomyces natalensis* HDMNTE-01 enhanced by response surface methodology. Prep Biochem Biotechnol. 2017;47:939–44.
9. Yue CP, Xu HT, Yu YY, Yu X, Yu M, Zhang C, et al. Improvement of Natamycin production by controlling the morphology of *Streptomyces Gilvosporeus* Z8 with microparticle Talc in seed preculture. J Chem Technol Biotechnol. 2021;96:1533–42.
10. Zeng X, Zeng HW, Meng Y, Xu D, Zhang B, Xin B, et al. Continuous Natamycin production by using immobilized *Streptomyces Gilvosporeus* Z8 via repeated batch culture. J Chem Technol Biotechnol. 2019;94:3116–24.
11. Liu SP, Yuan PH, Wang YY, Liu XF, Zhou ZX, Bu QT, et al. Generation of the Natamycin analogs by gene engineering of Natamycin biosynthetic genes in *Streptomyces chattanoogensis* L10. Microbiol Res. 2015;173:25–33.
12. Yuan HL, Zhou Y, Lin YP, Tu R, Guo YF, Zhang YY, et al. Microfluidic screening and genomic mutation identification for enhancing cellulase production in *Pichia pastoris*. Biotechnol Biofuels. 2022;15:50.
13. Sun JR, Li JL, Yao LL, Zheng YY, Yuan JF, Wang DH, et al. UV-ARTP-DES compound mutagenesis breeding improves Natamycin production of *Streptomyces hygroscopicus* HW-2 and reveals transcriptional changes by RNA-seq. Food Sci Biotechnol. 2023;32:341–52.
14. Zong GL, Cao GX, Fu J, Zhang PP, Chen X, Yan WX, et al. MacRS controls morphological differentiation and Natamycin biosynthesis in *Streptomyces Gilvosporeus* F607. J Ind Microbiol Biotechnol. 2022;262:127077.
15. Wang M, Wang S, Zong G, Hou Z, Liu F, Liao D, et al. Improvement of Natamycin production by cholesterol oxidase overexpression in *Streptomyces Gilvosporeus*. J Microbiol Biotechnol. 2016;26:2417.
16. Tao Z, Wang Y, Zheng H, Tao M. Improvement of Natamycin production in an industrial strain by heterologous expression of the AfsRS global regulatory genes. Chin J Biotechnol. 2015;31:744–51.
17. Ega SL, Drendel G, Petrovski S, Egidi E, Franks AE, Muddada S. Comparative analysis of structural variations due to genome shuffling of *Bacillus subtilis* VS15 for improved cellulase production. Int J Mol Sci. 2020;21:1299.
18. Alzahrani NH, El-Bondkly AA, El-Gendy M, El-Bondkly AM. Enhancement of undecylprodigiosin production from marine endophytic Recombinant strain *Streptomyces* Sp. ALAA-R20 through low-cost induction strategy. J Appl Genet. 2021;62:165–82.
19. Xu S, Ren N, Liu J, Wu Y, Yuan G. Improvement of Vincamine production of endophytic fungus *Aspergillus* Sp. through inactivated protoplast fusion. Int Microbiol. 2020;23:441–51.
20. Bruna RE, Kendra CG, Pontes MH. Coordination of phosphate and magnesium metabolism in bacteria. In: Razzaque MS, editor. Phosphate metabolism. Cham: Springer; 2022. pp. 135–50.
21. Mendes MV, Tunca S, Antón N, Recio E, Sola-Landa A, Martín J, et al. The two-component phoR-phoP system of *S. natalensis*: inactivation or deletion of PhoP reduces the negative phosphate regulation of Pimaricin biosynthesis. Metab Eng. 2007;9:217–27.
22. Tian Q, Li W, Li J, Xiao Y, Wu B, Wang Z, et al. Towards Understanding PRPS1 as a molecular player in immune response in yellow drum (Nibea albiflora). Int J Mol Sci. 2022;23:6475.
23. Sun X, Li X, Zhang Y, Li W, Li J, Wang Y, et al. Detection method optimization, content analysis and stability exploration of Natamycin in wine. Food Chem. 2016;194:928–37.
24. Aparicio JF, Colina AJ, Ceballos E, Martín JF. The biosynthetic gene cluster for the 26-membered ring polyene macrolide Pimaricin: a new polyketide synthase organization encoded by two subclusters separated by functionalization genes. J Biol Chem. 1999;274:10133–9.
25. Martín JF, Aparicio JF. Enzymology of the polyenes Pimaricin and Candicidin biosynthesis. Methods Enzymol. 2009;459:215–42.
26. Du YL, Li SZ, Zhou Z, Chen SF, Fan WM, Li YQ. The pleiotropic regulator AdpAch is required for Natamycin biosynthesis and morphological differentiation in *Streptomyces chattanoogensis*. Microbiology. 2011;157:1300–11.
27. Li P, Lin P, Zhao Z, Li Z, Liu Y, Huang C, et al. Gene co-expression analysis reveals transcriptome divergence between wild and cultivated sugarcane under drought stress. Int J Mol Sci. 2022;23:569.
28. Rang J, Xia Z, Shuai L, Cao L, Liu Y, Li X, et al. A TetR family transcriptional regulator, SP_2854 can affect the butenyl-spinosyn biosynthesis by regulating glucose metabolism in *Saccharopolyspora spinosa*. Microb Cell Fact. 2022;21:83.
29. Chen SSY, Ning B, Song JW, Yang ZN, Zhou L, Chen Z, et al. Enhanced Pentose phosphate pathway activity promotes pancreatic ductal adenocarcinoma progression via activating YAP/MMP1 axis under chronic acidosis. Int J Biol Sci. 2022;18:2304–16.
30. Bertels LK, Fernández Murillo L, Heinisch JJ. The Pentose phosphate pathway in yeasts—more than a poor cousin of Glycolysis. Biomolecules. 2021;11:725.
31. Jia B, Yin J, Li X, Li Y, Yang X, Lan C, et al. Increased lipids in *Chlamydomonas reinhardtii* by multiple regulations of DOF, LACS2, and CIS1. Int J Mol Sci. 2022;23:10176.
32. Saito M, Konishi M, Miyagi A, Sakuraba Y, Kawai-Yamada M, Yanagisawa S. Arabidopsis nitrate-induced aspartate oxidase gene expression is necessary to maintain metabolic balance under nitrogen nutrient fluctuation. Commun Biol. 2022;5:432.
33. Martín-Martín S, Rodríguez-García A, Santos-Beneit F, Franco-Domínguez E, Sola-Landa A, Martín JF. Self-control of the PHO Regulon: the PhoP-dependent protein PhoU negatively controls expression of genes of PHO Regulon in *Streptomyces coelicolor*. J Antibiot (Tokyo). 2017;70:1063–9.

34. Fernández-Martínez LT, Santos-Beneit F, Martín JF. Is PhoR-PhoP partner fidelity strict? PhoR is required for the activation of the Pho Regulon in *Streptomyces coelicolor*. Mol Genet Genomics. 2012;287:565–73.
35. Bruna RE, Kendra CG, Pontes MH. An intracellular phosphorus-starvation signal activates the PhoB/PhoR two-component system in *Salmonella enterica*. mBio. 2024;15:e01642–24.
36. Xu Y, You D, Yao L, Chu X, Ye B. Phosphate regulator PhoP directly and indirectly controls transcription of the erythromycin biosynthesis genes in *Saccharopolyspora Erythraea*. Microb Cell Fact. 2019;18:555739.
37. Zheng Y, Sun C, Fu Y, Chen X, Li YQ, Mao X. Dual regulation between the two-component system phorp and adpa regulates antibiotic production in *Streptomyces*. J Ind Microbiol Biotechnol. 2019;46:725–37.
38. Zhang B, Chen Y, Jiang SX, Cai X, Huang K, Liu ZQ, et al. Comparative metabolomics analysis of amphotericin B high-yield mechanism for metabolic engineering. Microb Cell Fact. 2021;20:1552.
39. Kobayashi S, Kawaguchi H, Shirai T, Ninomiya K, Takahashi K, Kondo A, et al. Automatic Redirection of carbon flux between Glycolysis and Pentose phosphate pathway using an oxygen-responsive metabolic switch in *Corynebacterium glutamicum*. ACS Synth Biol. 2020;20:00493.
40. Qin N, Li L, Ji X, Li X, Zhang Y, Larsson C, et al. Rewiring central carbon metabolism ensures increased provision of acetyl-CoA and NADPH required for 3-OH-propionic acid production. ACS Synth Biol. 2020;9:3236–44.
41. Masi A, Mach R, Mach-Aigner AR. The Pentose phosphate pathway in industrially relevant fungi: crucial insights for bioprocessing. Appl Microbiol Biotechnol. 2021;105:4017–31.
42. Lejeune C, Sago L, Cornu D, Redeker V, Virolle MJ. A proteomic analysis indicates that oxidative stress is the common feature triggering antibiotic production in *Streptomyces clavuligerus* and in the Δphop mutant of *Streptomyces coelicolor*. Front Microbiol. 2022;12:813993.
43. Su Y, Gao L, Li C, Wang L, Zhou H, Zhang C, et al. Regulation mechanism and bioactivity characteristic of surfactin homologues with C14 and C15 fatty acid chains. Microb Cell Fact. 2024;23:94.
44. Cai D, Zhu J, Zhu S, Lu Y, Zhang B, Lu K, et al. Metabolic engineering of main transcription factors in carbon, nitrogen, and phosphorus metabolisms for enhanced production of bacitracin in *Bacillus licheniformis*. ACS Synth Biol. 2019;8:866–75.
45. Sun Y, Zou H, Li X, Xu S, Liu C. Plasma metabolomics reveals metabolic profiling for diabetic retinopathy and disease progression. Front Endocrinol. 2021;12:757088.
46. Jha V, Bombaywala S, Purohit H, Dafale N. Differential colonization and functioning of microbial community in response to phosphate levels. J Environ Manage. 2022;321:115856.
47. Santos-Beneit F, Martín JF. Vancomycin resistance in *Streptomyces coelicolor* is phosphate-dependent but is not mediated by the PhoP regulator. J Glob Antimicrob Resist. 2013;1:109–13.
48. Santos-Beneit F. Genome sequencing analysis of *Streptomyces coelicolor* mutants that overcome the phosphate-depending Vancomycin lethal effect. BMC Genomics. 2018;19:457.
49. Santos-Beneit F, Rodríguez-García A, Sola-Landa A, Martín JF. Cross-talk between two global regulators in *Streptomyces*: PhoP and AfsR interact in the control of AfsS, PstS and phorp transcription. Mol Microbiol. 2009;72:53–68.
50. Ordóñez-Robles M, Santos-Beneit F, Rodríguez-García A, Martín JF. Analysis of the Pho Regulon in *Streptomyces tsukubaensis*. Microbiol Res. 2017;205:80–7.
51. Sola-Landa A, Moura RS, Martín JF. The two-component PhoR-PhoP system controls both primary metabolism and secondary metabolite biosynthesis in *Streptomyces lividans*. Proc Natl Acad Sci U S A. 2003;100:6133–8.

Publisher's note